Observation of the Stark-Tuned Förster Resonance between Two Rydberg atoms

I. I. Ryabtsev,* D. B. Tretyakov, I. I. Beterov, and V. M. Entin
Institute of Semiconductor Physics, Prospekt Lavrentyeva 13, 630090 Novosibirsk, Russia
(Dated: 18 February 2010)

Cold atoms in highly excited Rydberg states are promising candidates to implement quantum logic gates of a quantum computer via long-range dipole-dipole interaction. Two-qubit gates require a controlled interaction of only two close Rydberg atoms. We report on the first spectroscopic observation of the resonant dipole-dipole interaction between two cold rubidium Rydberg atoms confined in a small laser excitation volume. The interaction strength was controlled by fine tuning of the Rydberg levels into a Förster resonance using the Stark effect. The observed resonance line shapes are in good agreement with numerical Monte-Carlo simulations.

PACS numbers: 32.80.Ee, 03.67.Lx, 32.70.Jz , 34.10.+x

Quantum computers are among of the most intriguing challenges for researchers in different areas of physics. As no fully working quantum computer has been reported yet, many approaches are being developed simultaneously [1,2]. One promising approach is a quantum computer based on neutral alkali-metal atoms trapped in optical lattices or dipole traps [2]. Each atom represents a qubit whose quantum states are the two hyperfine sublevels of the ground state.

The most challenging task with neutral atoms is to implement the two-qubit quantum logic gates needed to entangle the qubits. Such gates require a controlled interaction between qubits separated by several microns. As ground-state atoms interact very weakly at such distances, it has been proposed [3,4] to excite atoms to high Rydberg states with principal quantum number $n \gg 1$. This provides strong dipole-dipole interaction (DDI) between qubits ($\sim n^4$) [5].

Two basic proposals consider a short-term DDI of two close Rydberg atoms [3] or laser excitation of only one Rydberg atom in a mesoscopic ensemble (dipole blockade) [4]. A combination of these ideas has resulted recently in the first implementation of the controlled-NOT quantum gate with fidelity 0.73 [6] and of the entanglement with fidelity 0.75 [7] using the dipole blockade at laser excitation of two Rydberg atoms separated by 10 or 4 μm. Both experiments actually employ quasiresonant dipole-dipole interaction at quasi-Förster resonance, instead of the Stark-tuned Förster resonance originally proposed in Ref. [4].

Förster resonant energy transfer appears due to DDI of the atoms excited to a level that lies midway between two other levels [8]. For some levels it can be precisely tuned with an electric field via the Stark effect [9]. Stark-tuned Förster resonance is more flexible in controlling the interaction strength, otherwise one needs to change the Rydberg states or interatomic distance. Stark-tuned Förster resonance is also advantageous as it allows for direct measurement of the interaction strength between two atoms by recording its spectrum in the electric-field scale and subtracting the nonresonant background signal [10]. However, such a resonance was never observed for two Rydberg atoms, to the best of our knowledge.

In this Letter we report on the first experimental observation of the Stark-tuned Förster resonance between a definite number (2−5) of closely spaced Rydberg atoms. Such a study is a prerequisite for future quantum gates that employ Förster resonances controlled with a weak dc electric field. In particular, line-shape analysis is important, as the resonance can be broadened by various sources of decoherence and thus may affect fidelity of quantum gates. Coherent or incoherent evolution of the interacting Rydberg atoms, while experiencing various decoherence processes, should be precisely investigated. Electrical control of the Förster resonance can be used to adjust the phase of the collective wave function in quantum phase gates or to implement the dipole blockade [11].

Experiments with few Rydberg atoms require special techniques for their manipulation and detection. We have developed a method to separately measure the signals from $N = 1-5$ of the detected Rydberg atoms [10]. Our technique uses a selective field ionization (SFI) detector [5] with a channel electron multiplier and relies on post-selecting the signals. In this work we applied it to cold Rb Rydberg atoms in a magneto-optical trap (MOT).

The Förster resonance under study is the resonant energy transfer $\mathrm{Rb}\left(37P_{3/2}\right) + \mathrm{Rb}\left(37P_{3/2}\right) \rightarrow \mathrm{Rb}\left(37S_{1/2}\right) + \mathrm{Rb}\left(38S_{1/2}\right)$ due to DDI of two or more Rb Rydberg atoms in a small laser excitation volume. The initial energy detuning $\Delta = \left[2E\left(37P_{3/2}\right) - E\left(37S_{1/2}\right) - E\left(38S_{1/2}\right)\right]/h$ in a zero electric field is 103 MHz; Δ becomes zero at 1.79 V/cm.

The experiments were performed with cold ^{85}Rb atoms in a MOT of standard configuration. Typically 10^5-10^6 atoms were trapped in a 0.5−0.6 mm diameter cloud. The electric field for SFI was formed by two stainless-steel plates with holes and meshes for passing the vertical laser cooling beams and the electrons to be detected. Channel electron multiplier output pulses from the $37S$ and ($37P$+$38S$) states were detected with two independent gates and sorted according to the number of detected Rydberg atoms N.

*Electronic address: ryabtsev@isp.nsc.ru

The excitation of Rb atoms to the $37P$ Rydberg state was realized in four steps: (i) $5S \rightarrow 5P_{3/2}$ with a 780 nm cw cooling laser; (ii) $5P_{3/2} \rightarrow 8S$ with a 615 nm pulsed Rh 6G dye laser; (iii) $8S \rightarrow (6P, 7P) \rightarrow 6S$ spontaneous cascade decay during 200 ns; and (iv) $6S \rightarrow 37P$ with a 743 nm pulsed Ti:sapphire laser. The pulsed lasers had a pulse width of 50 ns at a repetition rate of 5 kHz.

A small Rydberg excitation volume was formed using a crossed-beam geometry [12]. The two pulsed laser beams were focused to a waist of 9−10 μm in diameter and intersected at right angles inside the cold atom cloud. The laser intensities were adjusted to obtain about one Rydberg atom excited per laser pulse on average. Numerical simulation for these intensities gave the effective volume of $\simeq$5800 μm^3 (a cubic volume of 18 μm in size).

Microwave spectroscopy was applied for diagnostics of the electromagnetic fields in the excitation volume: dc electric field was calibrated with 0.2% uncertainty using Stark spectroscopy of the microwave transition $37P_{3/2} \rightarrow 37S_{1/2}$; MOT magnetic field was not switched off, but the microwave probing allowed us to align the excitation point to a nearly zero magnetic field [12].

We observed formation of $2-5$ ions due to photoionization at laser excitation. The ions were removed by a 5 V/cm electric-field pulse of 2 μs duration. After this pulse, the electric field decreased to a variable value of 1.7−2.1 V/cm and acted for 3 μs until the SFI pulse.

The spectra of the Förster resonances were separately recorded for various N=1−5. The measured signals are the fraction of atoms in the final $37S$ state

$$S_N = \frac{n_N\,(37S)}{n_N\,(37P) + n_N\,(37S) + n_N\,(38S)}, \qquad (1)$$

where $n_N\,(nL)$ is the total number of nL Rydberg atoms detected by SFI during the accumulation time for the particular case of N detected Rydberg atoms. Upon complete coherent transfer from the $37P$ state to the $37S$ and $38S$ states, S_N reaches a maximum value of 0.5, as both final states are populated with equal probability. An incoherent transfer to those states leads to $S_N \leq 0.25$.

The Förster resonance spectra recorded for N=1−5 after a free interaction time t_0=3 μs are shown in Fig. 1(a). Each point was averaged over $\simeq 10^5$ laser pulses. The laser polarization was oriented along the dc electric field to provide excitation of only the $37P_{3/2}(|M_J|=1/2)$ atoms from the intermediate $6S$ state. In this case a single resonance at 1.79 V/cm is observed. The height and width of the resonance grow with N, as expected from simple theoretical considerations [10]. However, precise comparison between theory and experiment should be based on an adequate theoretical model for few Rydberg atoms. In what follows, we calculate the theoretical spectra and then compare them with the experiment.

The first item to be discussed is, When we observe the spectrum S_N for N detected Rydberg atoms, does it really correspond to the spectrum ρ_N for the interaction of exactly N atoms? In our previous paper [10] we have

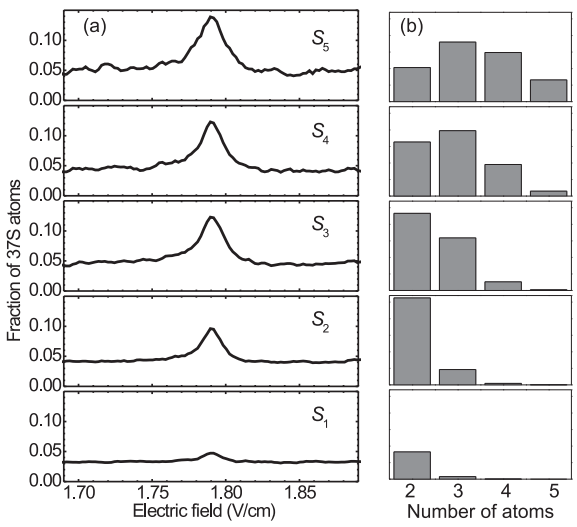

FIG. 1: (a) Experimental spectra $S_1 - S_5$ of the Förster resonance $\mathrm{Rb}\left(37P_{3/2}\right) + \mathrm{Rb}\left(37P_{3/2}\right) \rightarrow \mathrm{Rb}\left(37S_{1/2}\right) + \mathrm{Rb}\left(38S_{1/2}\right)$ for 1−5 detected Rydberg atoms. (b) Theoretical probability distributions given by Eqs. (2) and (3) for the number of actually interacting Rydberg atoms.

shown that for an ideal SFI detector the signal S_N indeed gives the true spectrum ρ_N. For the nonideal detector, which detects fewer atoms than have actually interacted, various ρ_i contribute to S_N to a degree that depends on the mean number of the detected Rydberg atoms. The spectra S_N are thus a mixture of the spectra from the larger numbers of actually interacting atoms $i \geq N$ [10]:

$$S_N = \rho + e^{-\bar{n}(1-T)} \sum_{i=N}^{\infty} \rho_i \frac{\left[\bar{n}\,(1-T)\right]^{i-N}}{(i-N)!}. \qquad (2)$$

Here ρ is a nonresonant background signal due to blackbody-radiation-induced transitions and background collisions, $\bar{n}$ is the mean number of Rydberg atoms excited per laser pulse, and T is the detection efficiency of the SFI detector. The mean number of Rydberg atoms detected per laser pulse is $\bar{n}T$. In our experiment it was measured to be $\bar{n}T = 0.65 \pm 0.05$. According to the method developed in Ref. [10], this value along with the measured relationship between the one- and two-atom resonance amplitudes $\alpha = (S_1 - \rho)\,/\,(S_2 - \rho) = 0.27 \pm 0.03$ gives the unknown values of $\bar{n} = [\alpha/\,(1-\alpha) + \bar{n}T] = 1.05 \pm 0.04$ and $T = (65 \pm 5)\,\%$.

Equation (2) cannot be directly used to describe S_N in Fig. 1(a) as the fourth excitation step uses a broadband laser radiation. The dipole blockade effect is avoided with such radiation, however unwanted excitation to both fine sublevels of the $37P$ state is produced. Atoms in the $37P_{1/2}$ state do not interact but contribute to the number of the detected atoms. This leads to an additional mixing of the multiatom spectra, which can be taken into account by replacing ρ_i in Eq.(2) with a convolution of the probability to excite $i \geq 2$ atoms in a laser shot and

then to find $k \geq 2$ of these in the interacting $37P_{3/2}$ state ($k \geq 2$ as we need at least two atoms to interact):

$$\rho_i \rightarrow \left[\sum_{k=2}^{i} \rho_k \left(p_{3/2}\right)^k \left(p_{1/2}\right)^{i-k} \frac{i\,!}{k\,!\,(i-k)!} \right]. \quad (3)$$

Here $p_{3/2}$ and $p_{1/2}$ are the relative probabilities to excite the $37P_{3/2}$ and $37P_{1/2}$ atoms. Calculations have shown that at our laser intensities the $6S \rightarrow 37P$ transition strongly saturates and these atoms are excited with almost equal probabilities of $p_{3/2} \approx 0.52$ and $p_{1/2} \approx 0.48$.

The resulting theoretical distributions over ρ_i, calculated with Eqs. (2) and (3) for various S_N, are presented as histograms in Fig. 1(b). These histograms show that the S_1 and S_2 spectra almost completely originate from the interaction of two Rydberg atoms. To the best of our knowledge, this is the first observation of the Stark-tuned Förster resonance for two Rydberg atoms, which is the central result of this Letter. The method used thus paves the way to a detailed investigation of two-atom interactions, even when the SFI detection efficiency is far below 1. In particular, the line-shape analysis is necessary to reveal the effective coherence time at the Förster resonance to characterize the future quantum gates.

For the line-shape analysis we need to calculate various ρ_i. We applied a simplified theoretical model that considered only interactions of Rydberg atoms in the identical $37P_{3/2}(|M_J|{=}1/2)$ state. The operator of the DDI between two such atoms a and b is then reduced to

$$\hat{V}_{ab} = \frac{\hat{d}_a \hat{d}_b}{4\pi\varepsilon_0} \left(\frac{1}{R_{ab}^3} - \frac{3\ Z_{ab}^2}{R_{ab}^5} \right), \quad (4)$$

where $\hat{d}_{a,b}$ are the z components of the dipole-moment operators of the two atoms, R_{ab} is the distance between the atoms, Z_{ab} is the z component of the vector connecting the two atoms (the z axis is chosen along the dc electric field), and ε_0 is the dielectric constant. We have performed numerical Monte-Carlo simulations for $i{=}2{-}5$ interacting Rydberg atoms, randomly positioned in a small cubic volume. In this approach, the time evolution of all possible quasimolecular states is obtained by numerically solving the Schrödinger equation. We accounted for all possible binary resonant interactions between i atoms, as well as the always-resonant exchange interactions that may broaden the resonance. The initial positions of i atoms were averaged over 500 random realizations. A similar approach was used in Ref. [13].

Figure 2 shows the results of our calculations for $2{-}5$ atoms interacting for $t_0{=}0.515$ μs and randomly positioned in a $18 \times 18 \times 18$ μm^3 cubic volume. The interaction time was chosen to fit the widths of the resonances in Fig. 1(a), while the volume corresponds to the conditions of our experiment. The respective Rydberg atoms density is low and varies in the $(3-9)\cdot 10^8$ cm^{-3} range. The short interaction time allowed us to simplify the calculations by ignoring the effective lifetimes ($30{-}40$ μs [14]),

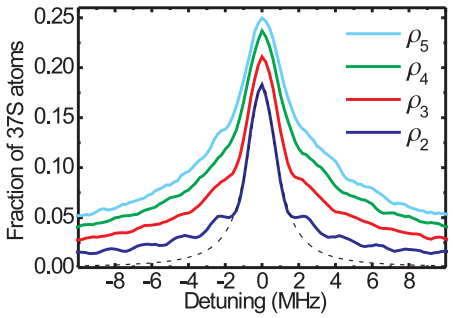

FIG. 2: (color online). Theoretical spectra ρ_i of the Förster resonance $\mathrm{Rb}\left(37P_{3/2}\right) + \mathrm{Rb}\left(37P_{3/2}\right) \rightarrow \mathrm{Rb}\left(37S_{1/2}\right) + \mathrm{Rb}\left(38S_{1/2}\right)$ obtained by numerical Monte-Carlo simulations for $i = 2-5$ atoms interacting for 0.515 μs and randomly positioned in a $18 \times 18 \times 18$ μm^3 cubic volume. The dashed line is an attempt of the Lorentz fit for ρ_2.

the motion of the atoms, and the hyperfine structure (for ^{85}Rb the estimated splittings are 380, 350, and 60 kHz for $37S$, $38S$, and $37P_{3/2}$ states, respectively). Accounting for the hyperfine structure is impossible due to the enormously large number of quasimolecular states, which in addition are strongly mixed by the electric field.

The theoretical spectra in Fig. 2 highlight several features. (i) At short interaction times the ultimate full width at half maximum (FWHM) is defined by the inverse interaction time $1/(t_0)$ ≈1.94 MHz for $i{=}2$. It is mainly a Fourier-transform limited width, which is larger than the estimated 0.3 MHz energy of DDI at an average distance of 10 μm. The probability for two atoms to interact at much shorter distances is low, and the resonance is narrow in spite of the spatial averaging. (ii) For $i > 2$ the resonances broaden due to increase in the average energy of DDI. Averaging over the atom positions forms a resonance with broad wings and a cusp on the top, which is similar to that observed in atomic beams [10,15]. (iii) The resonance amplitude $\rho_i\,(\Delta = 0)$ tends to saturate at the 0.25 value. This is due to the loss of coherence and washing out of the Rabi-like population oscillations upon spatial averaging. (iv) A dashed line in Fig. 2 is an attempt to fit the ρ_2 spectrum with a Lorentz profile. It is seen that when we match the central part, the resonance wings are much broader than the Lorentz ones, due to rare interactions at very short distances. The commonly used Lorentz fit is thus inadequate for precise comparison between theory and experiment, especially when a constant background signal is present in the experimental spectra.

Now we are able to analyze the line shapes in Fig. 1(a). In the S_1 spectrum, the FWHM in the electric-field scale is 16.4 ± 0.3 mV/cm, which corresponds to 1.94 ± 0.04 MHz. As the S_1 spectrum does not saturate, its width is defined by the effective interaction time that should be 0.515 μs according to theory. This time is shorter than $t_0{=}3$ μs we set up in the experiment. The reasons for this discrepancy can be understood as

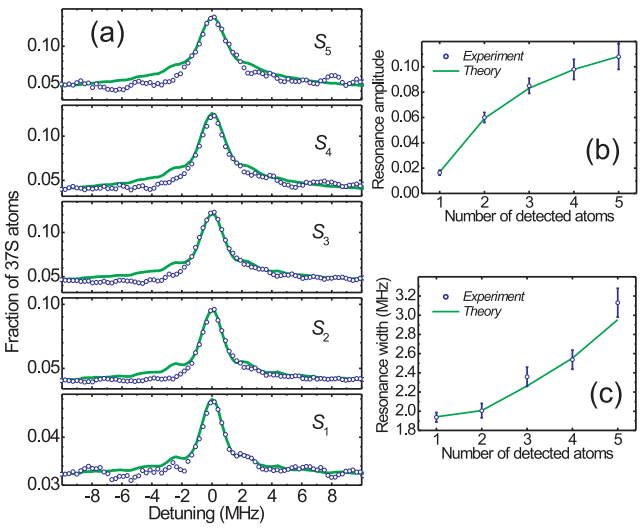

FIG. 3: (color online). (a) Comparison between theoretical (solid lines) and experimental (open circles) spectra of the Förster resonance. Theory uses the spectra of Fig. 2 and takes into account the mixing of these spectra due to finite detection efficiency and excitation of the noninteracting $37P_{1/2}$ atoms. Experiment corresponds to Fig. 1(a). (b) Theory and experiment for the resonance amplitude. (c) Theory and experiment for the resonance width.

follows. The free interaction time contributes about 0.3 MHz. The overall hyperfine structure contributes another 0.8 MHz. The inhomogeneous MOT magnetic field gives about 0.2 MHz. The remaining 0.7 MHz can be attributed to the parasitic ac electric fields of 5−6 mV/cm due to stray fields and ground loops. This analysis also agrees with the width of the microwave spectrum observed in the 1.79 V/cm electric field.

Our Monte-Carlo simulations have shown that all above broadenings can be accounted for by simply reducing the interaction time to 0.515 μs instead of 3 μs. A possible explanation is that any small level splitting, which is unresolved in the observed spectrum, adds to the total resonance width. As the resonance width is given by the inverse effective interaction time, this time should decrease when the splitting is taken into account. We conclude that the unresolved hyperfine, Zeeman, and Stark structures of the Förster resonance lead to a decrease of the effective interaction time and are thus the main sources of decoherence. Fast quantum gates should be implemented at much shorter interaction times.

The final theoretical spectra are shown as solid lines in Fig. 3(a). The open circles are the experimental data of Fig. 1(a) in the detuning scale. The nonresonant background level was added to the theory in order to fit the experiment at the far wings of the resonance and to correctly determine the resonance height. Figure 3(a) demonstrates the good agreement between the theoretical and experimental line shapes for all N. The wings of the experimental two-atom spectra S_1 and S_2 even reproduce some of the coherent features due to population oscillations. The slight asymmetry in the red-detuned wing is attributed to the nonsharp edges of the electric-field switching in the experiment. The resonance amplitude saturates at about 0.125 value [Fig.3(b)] instead of 0.25, because half of the Rydberg atoms are excited to the noninteracting $37P_{1/2}$ state. The dependence of the amplitude on N shows the good agreement between theory and experiment. The experimental dependence of the resonance FWHM on N is also close to theory [Fig.3(c)].

To conclude, we have observed for the first time the Förster resonance between two Rydberg atoms. Although the atom positions were not fixed, the interaction strength, the signal-to-noise ratio, and the spectral resolution were large enough for the line-shape analysis. The line shape agrees well with theory, showing that the two-atom interactions are controlled by an electric field in a predictable way. This is an important step towards implementation of the electrically controlled neutral-atom quantum gates. The next step should be the observation of coherent population oscillations at the Förster resonance, which is necessary for quantum phase gates [16].

We appreciate fruitful discussions with E. Arimondo and M. Saffman. This work was supported by the RFBR (Grants No. 09-02-90427 and No. 09-02-92428) jointly with the Consortium EINSTEIN, by the Russian Academy of Sciences, and by the Dynasty Foundation.

[1] A. Galindo and M. A. Martin-Delgado, Rev. Mod. Phys. **74**, 347 (2002).
[2] J. J. Garcia-Ripoll, P. Zoller, and J. I. Cirac, J. Phys. B **38**, S567 (2005).
[3] D. Jaksch *et al.*, Phys. Rev. Lett. **85**, 2208 (2000).
[4] M. D. Lukin *et al.*, Phys. Rev. Lett. **87**, 037901 (2001).
[5] T. F. Gallagher, *Rydberg Atoms* (Cambridge University Press, Cambridge, England, 1994).
[6] L. Isenhower *et al.*, Phys. Rev. Lett. **104**, 010503 (2010).
[7] T. Wilk *et al.*, Phys. Rev. Lett. **104**, 010502 (2010).
[8] K. A. Safinya *et al.*, Phys. Rev. Lett. **47**, 405 (1981).
[9] A. Tauschinsky *et al.*, Phys. Rev. A **78**, 063409 (2008); T. J. Carroll *et al.*, Phys. Rev. A **73**, 032725 (2006); K. Afrousheh *et al.*, Phys. Rev. A **74**, 062712 (2006).
[10] I. I. Ryabtsev *et al.*, Phys. Rev. A **76**, 012722 (2007); Erratum: Phys. Rev. A **76**, 049902(E) (2007).
[11] T. Vogt *et al.*, Phys. Rev. Lett. **97**, 083003 (2006).
[12] D. B. Tretyakov *et al.*, JETP **108**, 374 (2009).
[13] S. Westermann *et al.*, Eur. Phys. J. D **40**, 37 (2006); B. Sun and F. Robicheaux, Phys. Rev. A **78**, 040701(R) (2008); K. C. Younge *et al.*, Phys. Rev. A **79,** 043420 (2009).
[14] I. I. Beterov *et al.*, Phys. Rev. A **79**, 052504 (2009).
[15] J. R. Veale *et al.*, Phys. Rev. A **54**, 1430 (1996).
[16] S. Osnaghi *et al.*, Phys. Rev. Lett. **87**, 037902 (2001).